Supplemental Figures and Tables

Title: **Functionally-defined Therapeutic Targets in Diffuse Intrinsic Pontine Glioma**

Authors: Catherine S. Grasso, Yujie Tang, Nathalene Truffaux, Noah E. Berlow, Lining Liu, Marie-Anne Debily, Michael J. Quist, Lara E. Davis, Elaine C. Huang, Pamelyn J Woo, Anitha Ponnuswami, Spenser Chen, Tessa B. Johung, Wenchao Sun, Mari Kogiso, Yuchen Du, Lin Qi, Yulun Huang, Marianne Hütt-Cabezas, Katherine E. Warren, Ludivine Le Dret, Paul S. Meltzer, Hua Mao, Martha Quezado, Dannis G. van Vuurden, Jinu Abraham, Maryam Fouladi, Matthew N. Svalina, Nicholas Wang, Cynthia Hawkins, Javad Nazarian, Marta M. Alonso, Eric H. Raabe, Esther Hulleman, Paul T. Spellman, Xiao-Nan Li, Charles Keller, Ranadip Pal, Jacques Grill, Michelle Monje

Figure S1: Integrated mutational landscape of DIPG drug target genes.

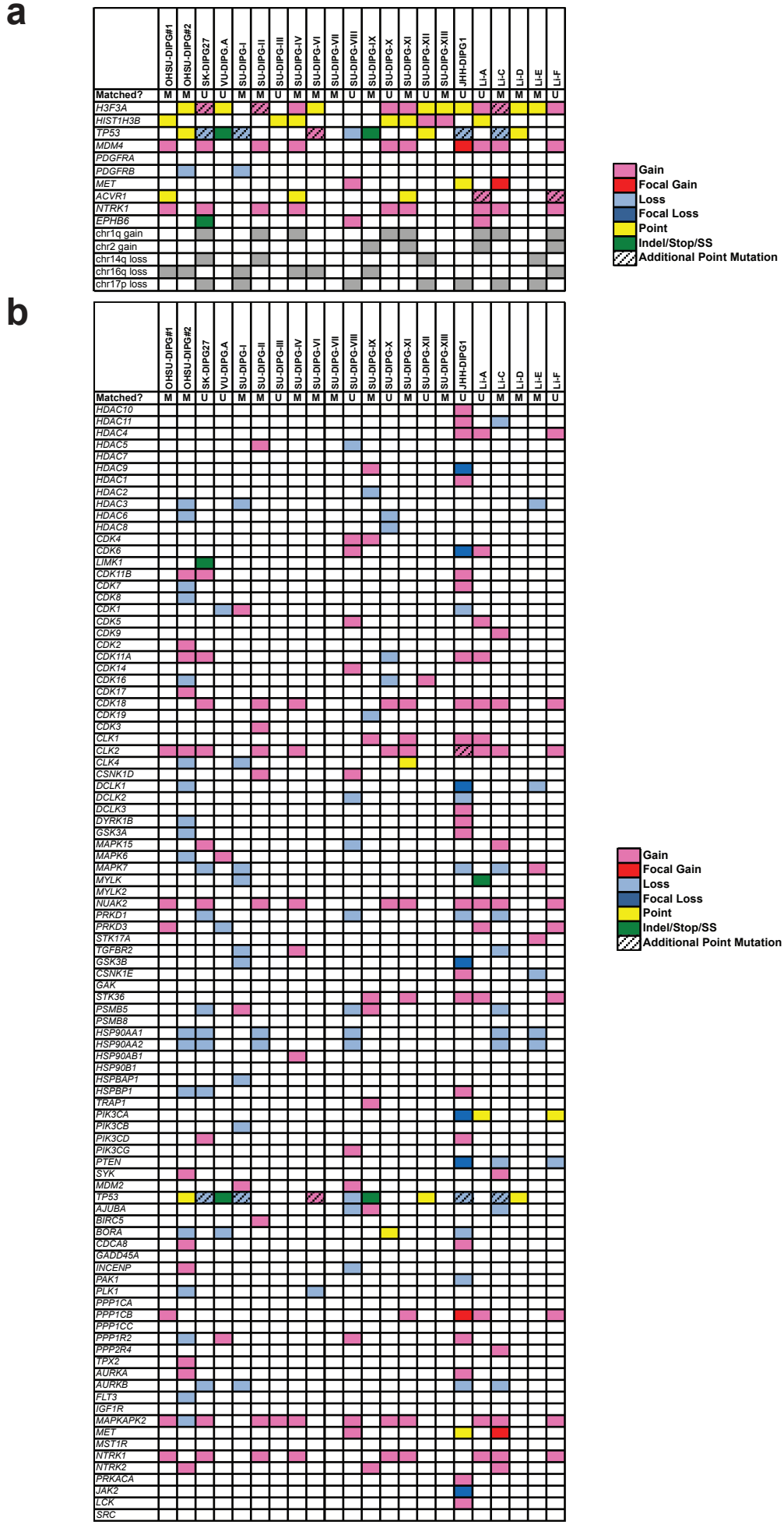

Supplementary Figure 1. Integrated mutational landscape of DIPG drug target genes. Exomes of 22 DIPG primary tumors were sequenced to identify somatic mutations and copy number alterations. Tumors with matched normal tissue are indicated by an "M", while those without matched normal tissue are indicated by a "U" in the second row of each heatmap. In (**a**), the mutation landscape has been restricted to highly-recurrent aberrations, while in (**b**), the mutation landscape has been restricted to genes targeted by top hits from the drug screen. Color key: pink = gain; red = focal gain; light blue = loss; royal blue = focal loss; yellow = point mutation; green = indel/stop mutation/ splice site mutation; rightward sloping hatched lines = additional point mutation.

Figure S2: Chemical screen 'hits' within the context of clinically-achievable serum drug levels.

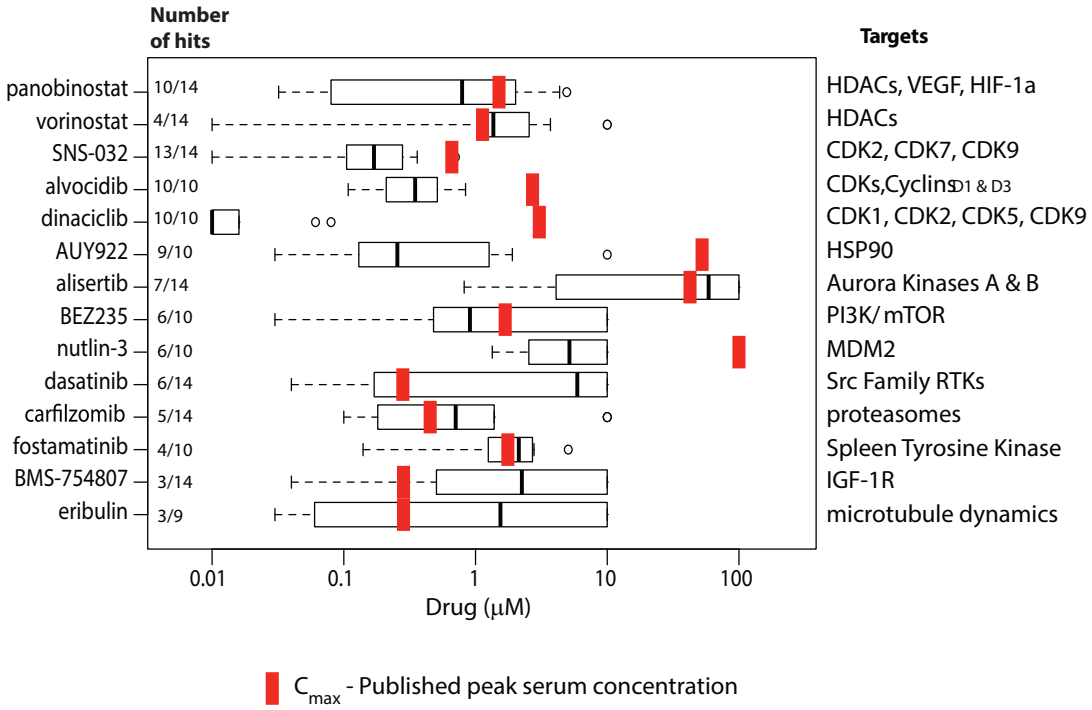

Supplementary Figure 2. Chemical screen 'hits' within the context of clinically-achievable serum drug levels. Box and whisker plot demonstrating the average absolute IC_{50} values ("box") +/- 1.5 standard deviation ("whiskers") for each of the top "hits", listed on the vertical axis, with concentration in μM on the horizontal axis. C_{max} (the peak serum concentration reported in the literature) for each drug is represented as a red bar. Open circles represent data points more than two standard deviations from the mean. The number of cell lines responding to each agent (out of the number of cells lines tested for that agent) at an IC_{50} value less than that drug's C_{max} is indicated to the left of the plot. For example, if 10 of 14 cell lines responded to panobinostat with an $IC_{50} < C_{max,}$ that is indicated as 10/14. Only those drugs that were "hits" in three or more cell lines are shown.

Figure S3: Gene expression and computational modeling highlight panobinostat as a promising treatment.

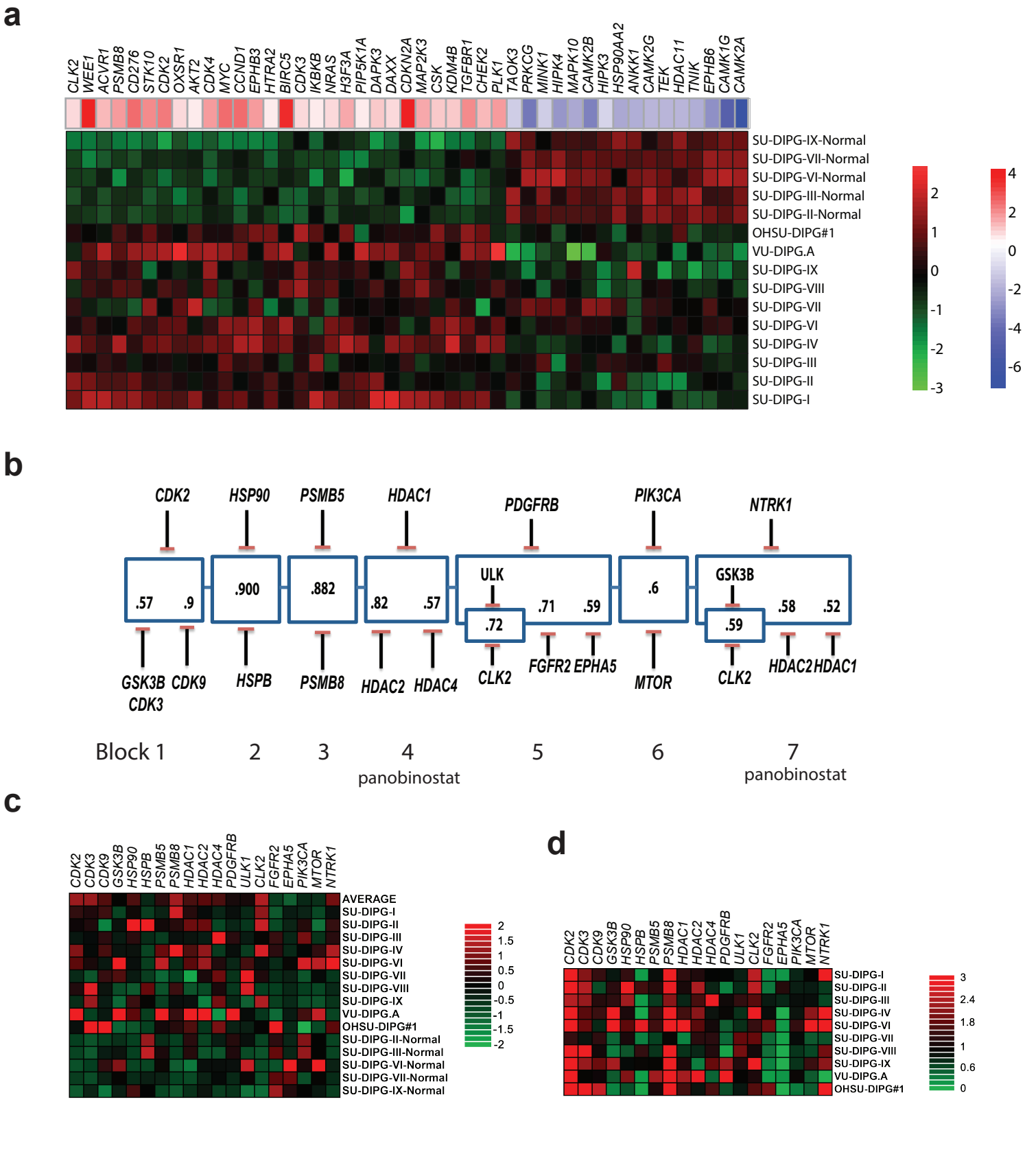

Supplementary Figure 3. Gene expression and computational modeling highlight panobinostat as a promising treatment. (**a**) Differentially expressed genes in DIPG primary tumors versus matched normal brain tissue. Heatmap of gene expression (RNAseq) data illustrating those genes with statistically significant differential expression using a t-test on the log of the expression and $p<0.01$ in primary tumor samples compared to normal brain tissue taken from unaffected areas of cerebral cortex. All primary tissue samples used in the RNAseq analysis were obtained at the time of autopsy; cases are described in Supplementary Table 1. Red and green heat map denotes differentially regulated genes, with red indicating up-regulation and green indicating down-regulation. Red and blue heatmap shows the log base 2 of the fold change calculated after taking the average of the tumors and the average of the normals. Gene names are on the horizontal axis and tumor sample names are on the vertical axis. (**b**) Computational modeling to identify salient gene targets: Tumor Inhibitor Map (TIM) circuit for the overall set of DIPG tumor sample drug responses. The circuit was derived from the complete set of 13 DIPG RNAseq-matched drug screen responses, and is a model for a general DIPG sample. Here, each block represents potential effective target inhibition combinations, *e.g.* inhibiting HDAC1 and HDAC2 or HDAC4 (block 4), would be an effective treatment. Shown here are the seven most relevant blocks (numbered below each block). Panobinostat inhibits HDACs in block 4 and block 7. The scores within each block represent the predicted efficacy of the block in terms of the expected sensitivity following inhibition of that block's gene targets. (**c**) Heatmap of z-values for protein targets identified by the DIPG TIM models: Heatmap of gene expression (RNAseq) data illustrating the relative expression z-values for the targets identified by the TIM model. Several of the targets have higher expression levels relative to other samples, and may indicate potential for differential drug sensitivity. Ex: SU-DIPG-IV and SU-DIPG-VI have higher NTRK1 expression relative to other samples, such as VU-DIPG.A. Correspondingly, crizotinib (an NTRK1 inhibitor) is highly effective on SU-DUPG-IV and SU-DIPG-VI, while VU-DIPG.A shows no sensitivity. **d**) Heatmap of differential expression between tumor and control samples for protein targets identified by the DIPG TIM models: Heatmap of the ratio of the gene expression (RNAseq) levels of the tumor samples to their matched normal or averaged group normal samples. The majority of targets are highly differentiated, even on samples not included in the TIM analysis. This may indicate a dependence on some of these overexpressed pathways for the cancerous samples. Example: cediranib (PDGFRB is one of its targets) is sensitive for VU-DIPG.A which may be due to the overexpression of PDGFRB (a target in the fifth TIM block). On the other hand, SU-DIPG-VI, which is not sensitive to cediranib has limited PDGFRB expression.

Figure S4: Validation of predicted synergy of PI3K and mTOR inhibition.

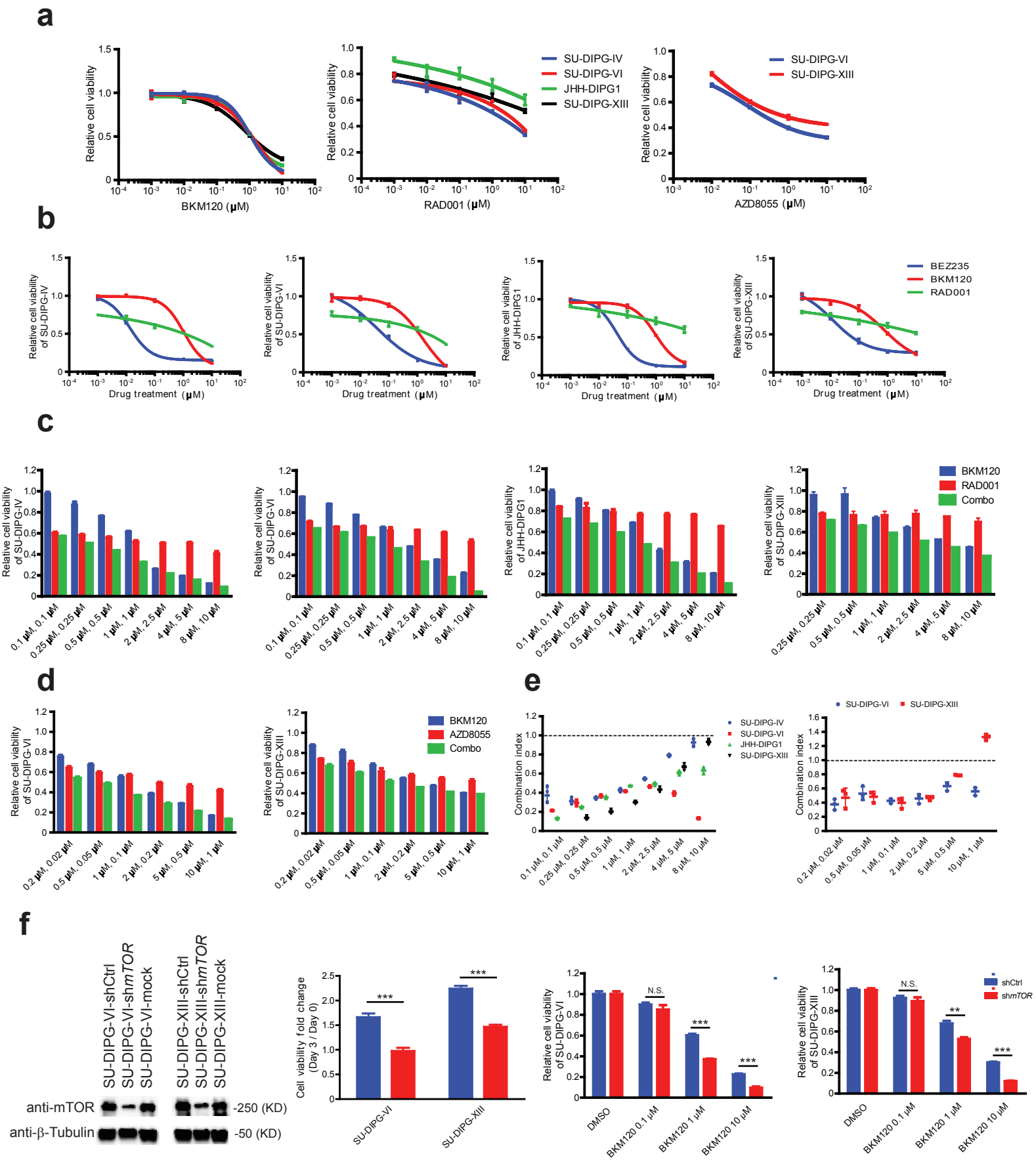

Supplementary Figure 4. Validation of predicted synergy of PI3K and mTOR inhibition. Most of the TIM circuit blocks can be hit with a single agent. To validate the predicted synergy of combinatorial PI3K and mTOR inhibition (block 6), we utilized pharmacological and genetic strategies. (**a)** DIPG lines were treated with the indicated drugs at 0.001/0.01/0.1/1/10 μM or 0.1% DMSO as control in at least triplicate. 72 hr post drug treatment, cell viabilities were assessed by using Celltiter Glo assay relative to 0.1% DMSO control. Data shown as mean ± SD. (**b)** Drug dosage curves of BEZ235 (PI3Ki+mTORi), BKM120 (PI3Ki) and RAD001 (mTORi) were aligned in parallel for each DIPG line respectively. (**c–d)** DIPG cells were seeded in 96-well plates and treated with the indicated two drugs individually or in combination at the indicated concentrations for 72 hr in at least triplicate. Cell viabilities were then assessed using Celltiter Glo assay relative to 0.1% DMSO control. Data shown as mean ± SD. (**e)** Combination index (CI) was calculated using CalcuSyn software from Biosoft. Data shown as mean ± SD. CI less than 1 was considered to be synergistic. (**f)** (left) Western blot analyses were performed to show the knockdown efficiency of sh*MTOR* at the protein level in DIPG cell lines. (middle) Cell viability fold change between Day 3 and Day 0 were calculated for DMSO treated shCtrl or sh*MTOR* infected cells in triplicate in two DIPG lines. Data shown as mean ± SD. (Right) DIPG cells infected with lentivirus expressing shCtrl or sh*MTOR* were seeded into 96-well plate for BKM120 drug treatment at doses of 0/0.01/0.1/1/10μM in triplicate for 72 hr, CelltiterGlo assay was performed to assess cell viability relative to DMSO control respectively. Data shown as mean ± SD. $^{**}P < 0.01$; $^{***}P < 0.001$; N.S. indicates $P > 0.05$.

Figure S5: Direct comparison of DIPG cell viability, proliferation and cell death in response to HDAC inhibitors panobinostat and vorinostat.

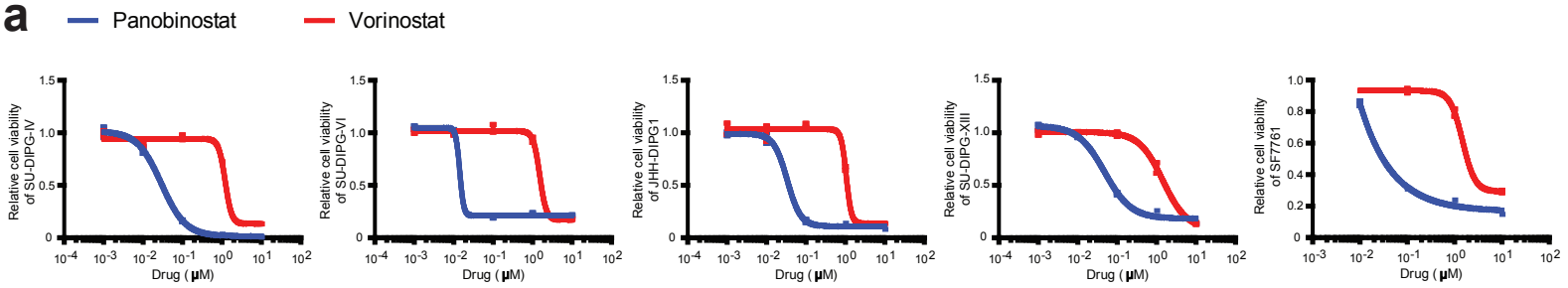

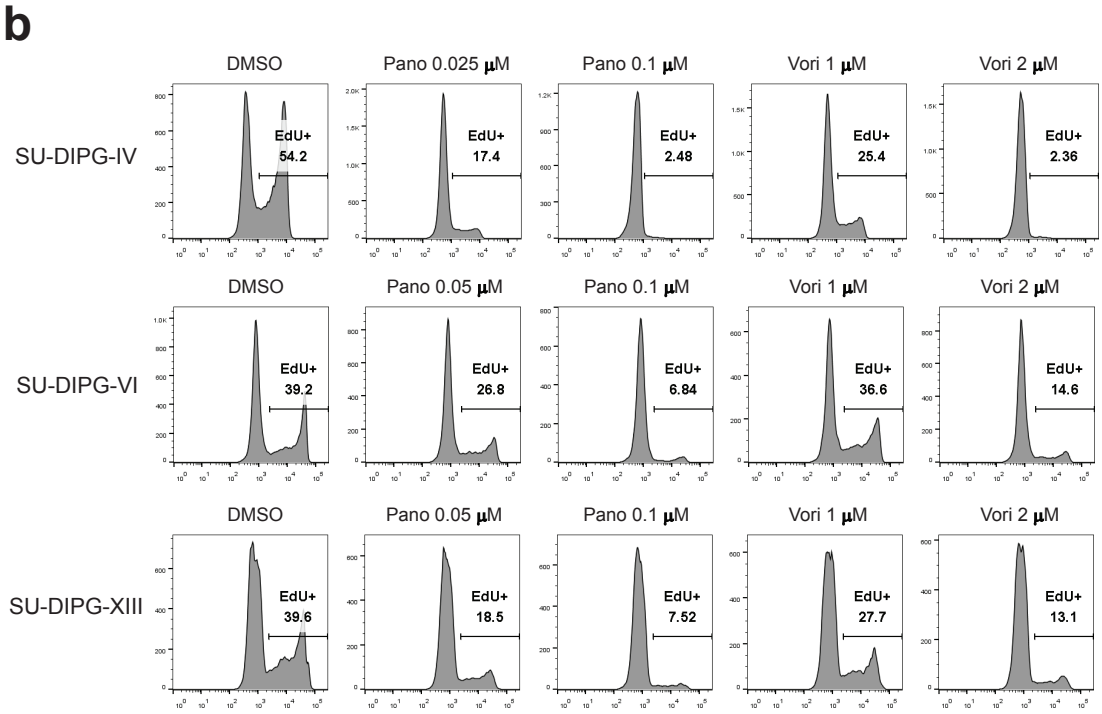

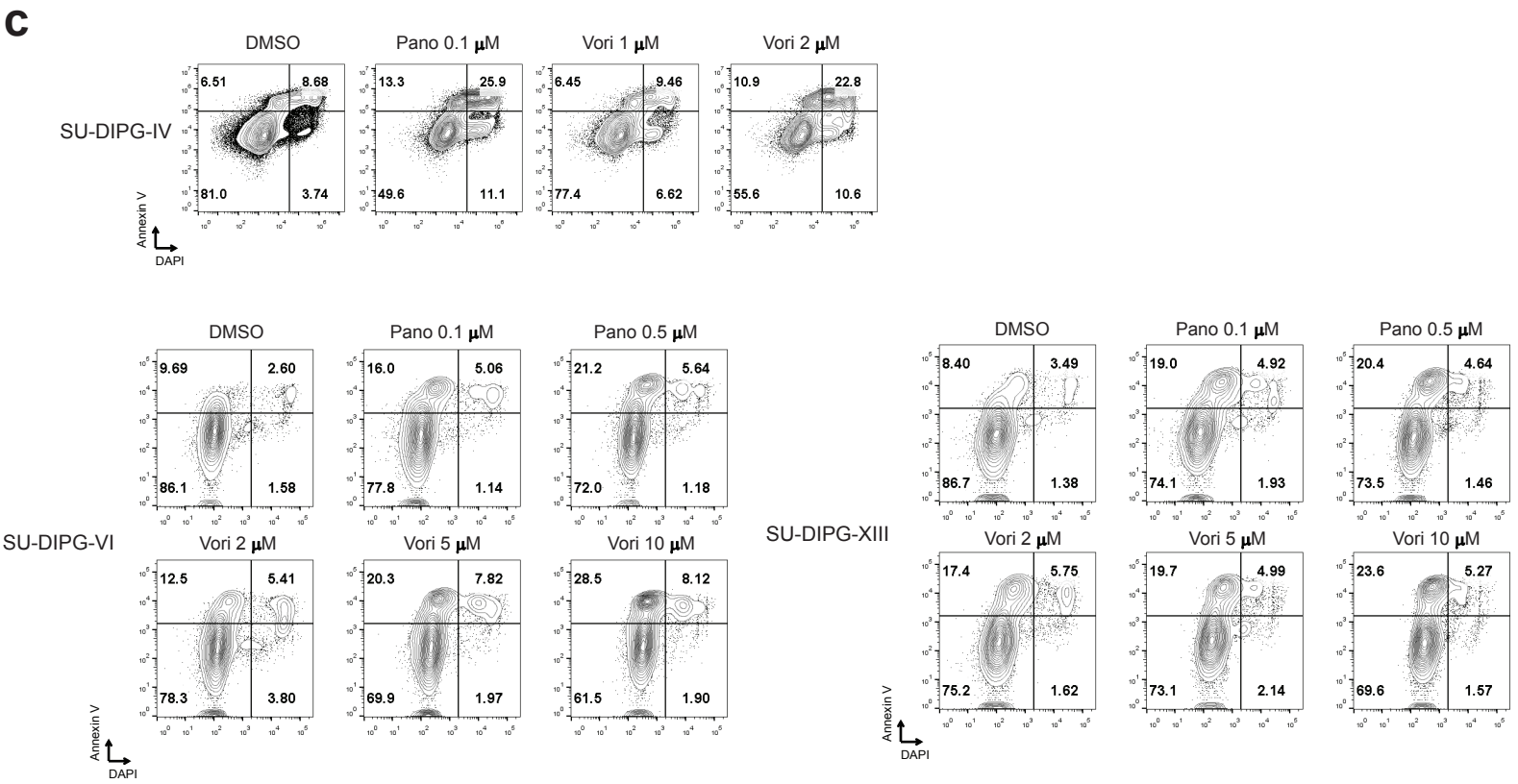

Supplementary Figure 5. Direct comparison of DIPG cell viability, proliferation and cell death in response to HDAC inhibitors panobinostat and vorinostat. Panobinostat is more potent than vorinostat. (**a**) Dose response curves of five DIPG cell cultures to panobinostst and vorinostat at increasing concentration, measured by CellTiterGlo at 72 hr. SU-DIPG-VI, SU-DIPG-XIII, JHH-DIPG1 and SF7761 exhibit the H3.3K27M mutation, SU-DIPG-IV exhibits the H3.1K27M mutation. (**b**) FACS analyses of cell proliferation (EdU incorporation, measuring *S*-phase) in response to panobinostat and vorinostat at the concentrations indicated. (**c**) FACS analyses of cell death as measured by Annexin-V and DAPI staining in response to panobinostat or vorinostat at the indicated concentrations. DIPG cell lines SU-DIPG-IV exhibits the H3.1K27M mutation; SU-DIPG-VI and SU-DIPG-XIII cell lines exhibit the H3.3K27M mutation.

Figure S6: DIPG cell proliferation and death in response to panobinostat or *HDAC* knock-down

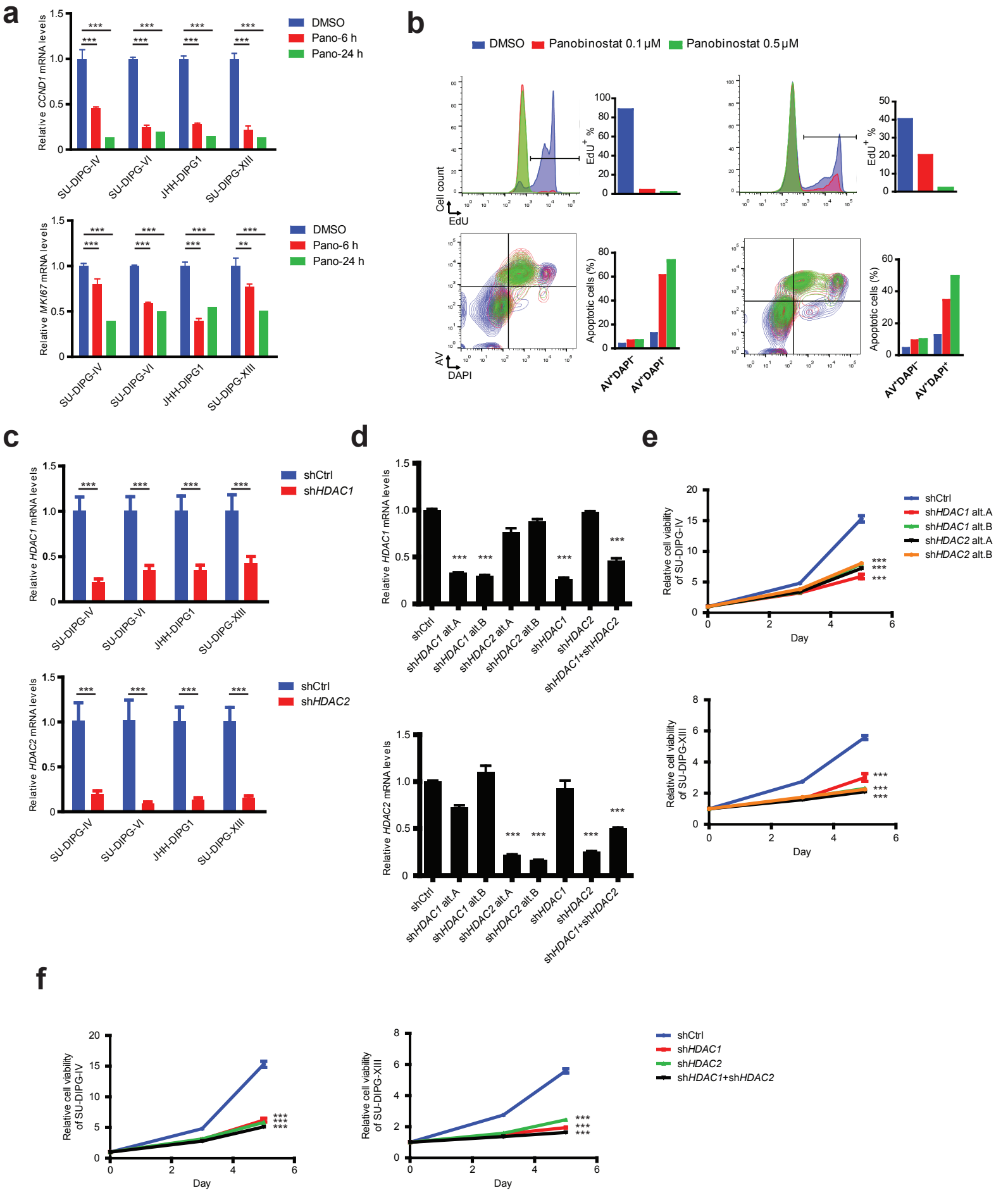

Supplementary Figure 6. DIPG cell proliferation and death in response to panobinostat or HDAC knock-down **(a)** Expression of proliferation genes *CCND1* and *MKI67* in response to panobinostat. DIPG cells were treated with 0.1 μM panobinostat for 6 or 24 hr before harvesting for RNA extraction. DMSO treated cells were collected in parallel as control. Quantitative RT-PCR analyses in quadruplicate were performed to show time course of *CCND1* (left) and *MKI67* (right) mRNA levels in response to 0.1 μM panobinostat treatment in DIPG cell lines. Data shown as mean ± SD. $^{**}P < 0.01$; $^{***}P < 0.001$. (**b**) FACS analyses of DIPG tumor cell proliferation and cell death. Top row: DIPG cells were treated with 0.1% DMSO vehicle or panobinostat at 0.1 or 0.5 μM for 24 hr and then incubated with 10 μM EdU for another 16 hours. Cells were then subjected to EdU FACS analysis to assess the proportion of cells in S-phase (EdU^+). Overlapping histogram plots of EdU FACS analyses are shown on the left; quantifications of EdU^+ cell population levels from each condition are shown in bar plots on the right for DIPG cell cultures SU-DIPG-IV (H3.1K27M mutant cell line) and JHH-DIPG1 (H3.3K27M mutant cell line). Bottom row: DIPG cells were treated with 0.1% DMSO or panobinostat at 0.1 or 0.5 μM for 48 hours and then examined using Annexin V, DAPI FACS analysis to assess the proportion of cells undergoing apoptosis. Overlapping plots of Annexin V/DAPI FACS analyses are shown on the left; quantifications of early apoptotic (AV^+DAPI^-) or late apoptotic (AV^+DAPI^+) cell population levels from each condition are shown in bar plots on the right for each cell line as above. (**c**) DIPG cells were infected with lentivirus expressing shCtrl, sh*HDAC1* or sh*HDAC2*. 48 hr following infection, 0.5 μg/ml Puromycin was added into culture to select positively infected cells for another 48 hr before the cells were harvested for RNA extraction. Quantitative RT-PCR analyses in quadruplicate were performed to show the knockdown efficiency of sh*HDAC1* (left) and sh*HDAC2* (right) at the mRNA level in DIPG cell lines. Data shown as mean ± SD. (**d**) DIPG cells infected with lentivirus expressing shRNAs as indicated were subjected to RNA extraction followed by quantitative RT-PCR analyses to measure the knockdown efficiency against *HDAC1* (left) or *HDAC2* (right). Two alternate sh*HDAC1* hairpins (sh*HDAC1* alt. A and B) and two alternate sh*HDAC2* hairpins (sh*HDAC2* alt. A and B) were tested to control for off-target effects. The combination of sh*HDAC1* and sh*HDAC2* was also tested in comparison to sh*HDAC1* or sh*HDAC2* individually. Data shown as mean ± SD. (**e**) DIPG cells infected with lentivirus expressing shCtrl, the two alternate sh*HDAC1* or the two alternate sh*HDAC2* were seeded in triplicate into 96-well plates and cell viability was assessed using the CelltiterGlo assay at 0, 3 and 5 days. Data are expressed relative to Day 0 and are shown as mean ± SD. **(f)** DIPG cells infected with lentivirus expressing sh*HDAC1* and sh*HDAC2* together or individually were seeded in triplicate into 96-well plates and cell viability was assessed using the CelltiterGlo assay at 0, 3 and 5 days. Data are expressed relative to Day 0 and are shown as mean ± SD respectively. Two-tailed t-tests were used in (**a**) and (**b**). Two-way ANOVAs were used in (**c**) and (**d**). $^{***}P < 0.001$

Figure S7: Top ranked differentially expressed genes in DIPG following panobinostat exposure.

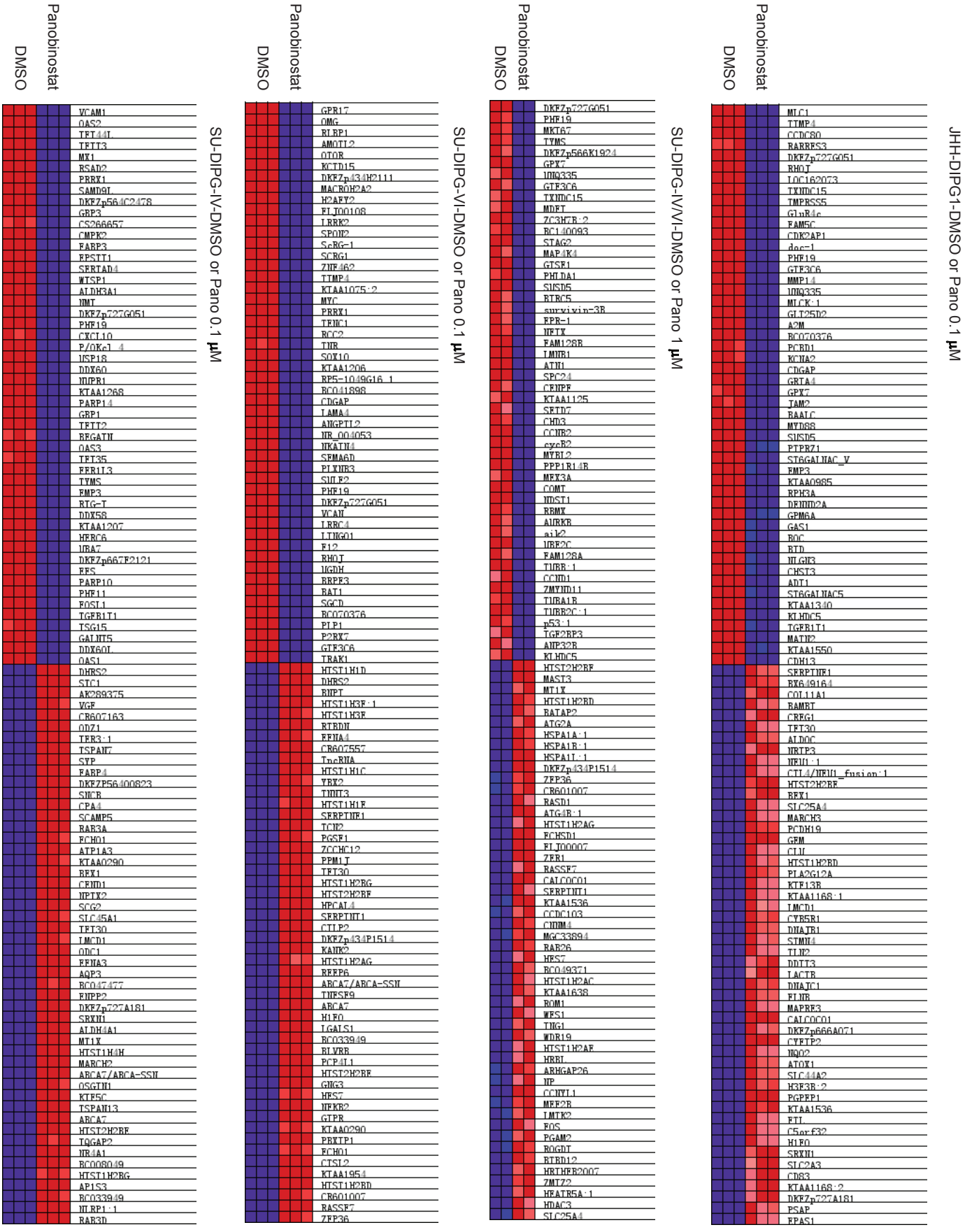

Supplementary Figure 7. Top ranked differentially expressed genes in DIPG following panobinostat exposure. Heatmap of the top ranked 50 down- and up-regulated genes in 4 sets of panobinostat treated and untreated DIPG cell lines (SU-DIPG-IV-DMSO or Pano 0.1μM, SU-DIPG-VI-DMSO or Pano 0.1μM, SU-DIPG-IV/IV-DMSO or Pano 1μM and JHH-DIPG1-DMSO or Pano 0.1μM) based on a signal-to-noise ratio (SNR) score generated by GSEA. Data are presented as row normalized. The data set presented at 1 μM panobinostat (SU-DIPG-IV/IV-DMSO or Pano 1 μM) represents RNAseq data from two cell lines (SU-DIPG-IV and SU-DIPG-VI). For 0.1 μM panobinostat studies, each of three cell lines (SU-DIPG-IV, SU-DIPG-VI and JHH-DIPG1) were treated in biological triplicate with 0 and 0.1 μM panobinostat.

Figure S8: Changes in DIPG gene expression following panobinostat exposure

a

Shared Enriched Gene Sets in DMSO
HELLER_HDAC_TARGETS_DN
HELLER_HDAC_TARGETS_SILENCED_BY_METHYLATION_DN
MARIADASON_REGULATED_BY_HISTONE_ACETYLATION_DN
PEART_HDAC_PROLIFERATION_CLUSTER_DN
ZHONG_RESPONSE_TO_AZACITIDINE_AND_TSA_DN

Shared Enriched Gene Sets in Panobinostat
HELLER_HDAC_TARGETS_UP
HELLER_HDAC_TARGETS_SILENCED_BY_METHYLATION_UP
MARIADASON_REGULATED_BY_HISTONE_ACETYLATION_UP
PEART_HDAC_PROLIFERATION_CLUSTER_UP
ZHONG_RESPONSE_TO_AZACITIDINE_AND_TSA_UP

b

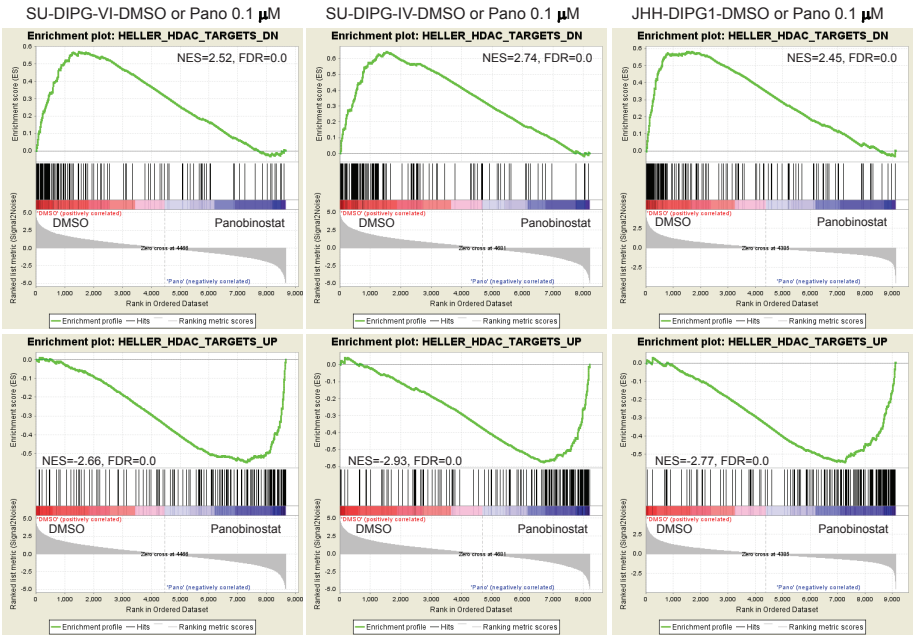

c

Enriched Gene Sets in DMSO, C2: curated gene sets
WONG_EMBRYONIC_STEM_CELL_CORE
SCHUHMACHER_MYC_TARGETS_UP
GOBERT_OLIGODENDROCYTE_DIFFERENTIATION_UP
WHITEFORD_PEDIATRIC_CANCER_MARKERS
ZHENG_GLIOBLASTOMA_PLASTICITY_UP
KEGG_CELL_CYCLE

Enriched Gene Sets in DMSO, C5: GO gene sets
MITOSIS
M_PHASE
M_PHASE_OF_MITOTIC_CELL_CYCLE
CHROMATIN_ASSEMBLY_OR_DISASSEMBLY
CHROMATIN_BINDING
CHROMOSOME_ORGANIZATION_AND_BIOGENESIS

d

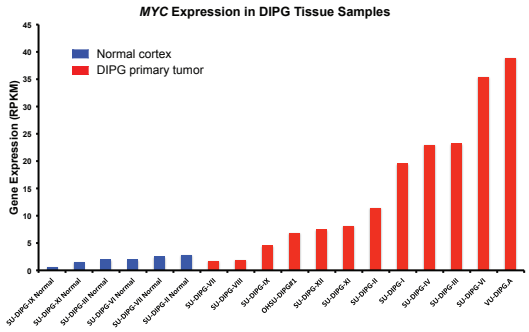

e

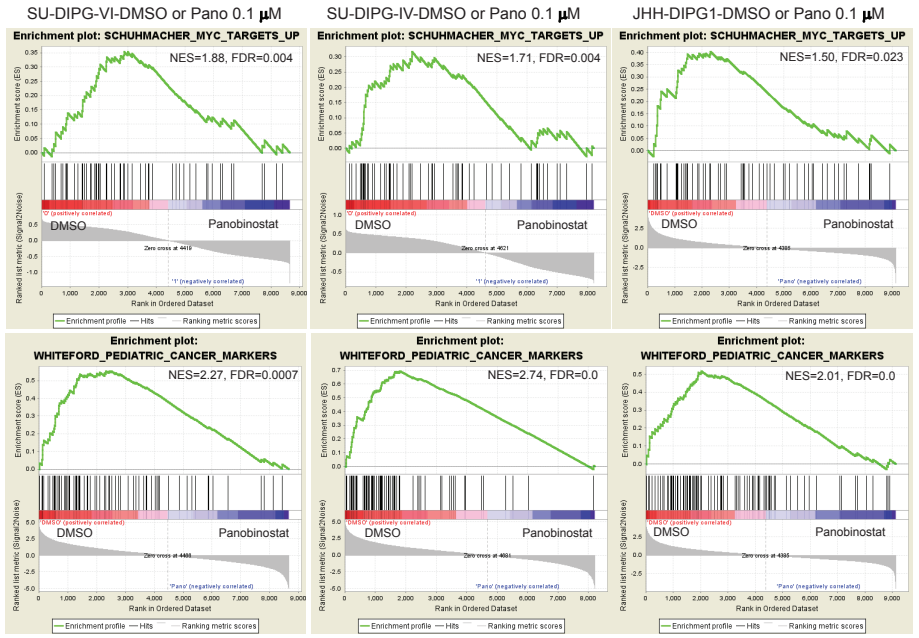

f

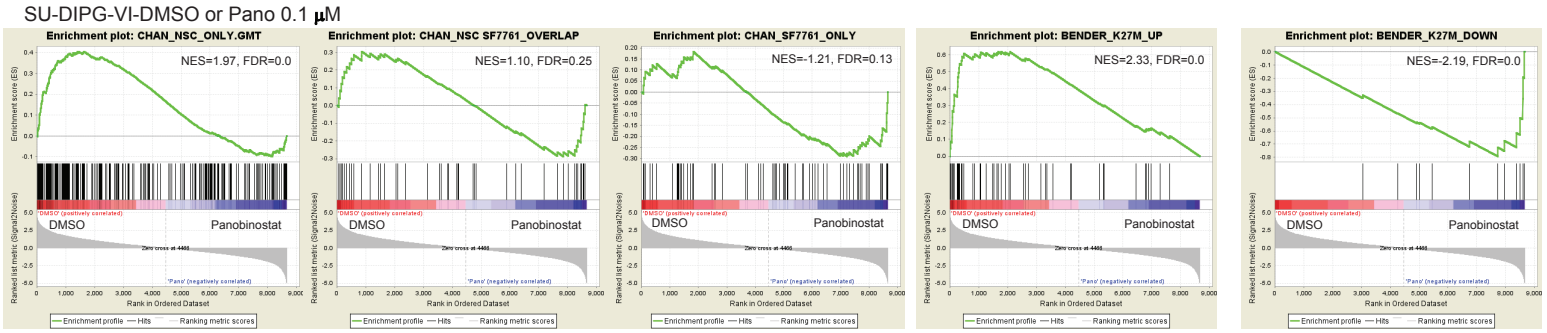

g

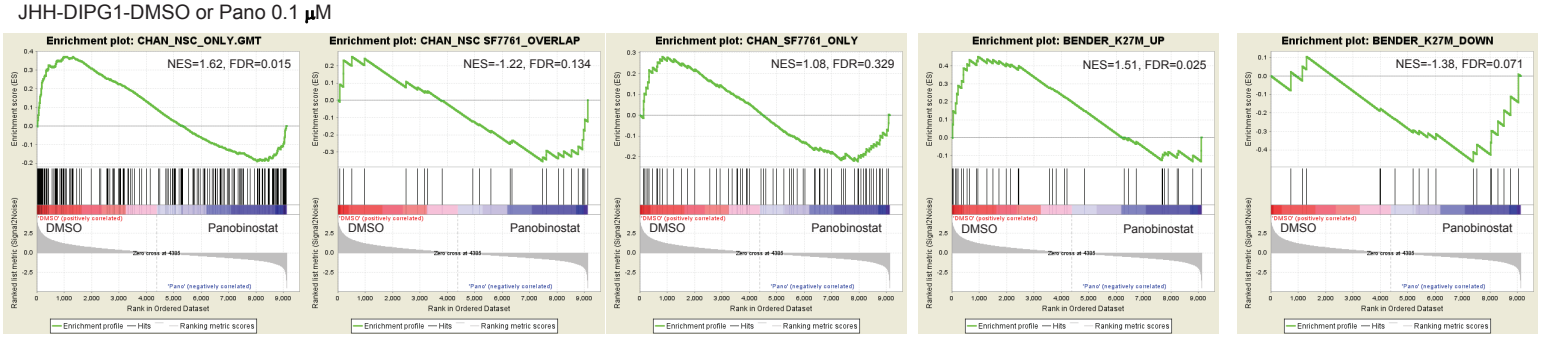

Supplementary Figure 8. Changes in DIPG gene expression following panobinostat exposure. (**a)** Shared enriched HDAC/HDACi-related gene sets from GSEA results of the 4 sets of panobinostat-treated DIPG cell lines. GSEA was performed against MSigDB-C2 (Curated gene sets) database and MSigDB-C5 (GO gene sets) database using 4 sets of gene profiles from panobinostat-treated DIPG cell lines. Significantly enriched gene sets were selected using cutoff of FDR$\leqslant$0.1. Venn diagram analysis was then used to identify the shared enriched gene sets. HDAC/HDACi-related gene sets were presented in either DMSO or Panobinostat-related samples. (**b)** GSEA showing down-regulation of HELLER_HDAC_TARGETS_DN gene set (genes down-regulated in at least one of three multiple myeloma (MM) cell lines by TSA) and up-regulation of HELLER_HDAC_TARGETS_UP gene set (genes up-regulated in at least one of three multiple myeloma (MM) cell lines by TSA) in panobinostat-treated samples. (**c**) Shared enriched cancer- or lineage-related gene sets from GSEA results of the 4 sets of panobinostat-treated DIPG cell lines. GSEA was performed against MSigDB-C2 (Curated gene sets) database and MSigDB-C5 (GO gene sets) database using 4 sets of gene profiles from panobinostat-treated DIPG cell lines. Significantly enriched gene sets were selected using cutoff of FDR $\leqslant$ 0.1. Venn diagram analysis was then used to identify the shared enriched gene sets. Representative cancer- or lineage-related gene sets enriched in DMSO samples were presented. (**d)** Gene expression levels of MYC in DIPG primary tumors (red) and normal cortex brain samples (blue) are represented in RPKM. (**e)** GSEA showing down-regulation of selected cancer- or MYC target-related gene sets in panobinostat-treated samples. (**f–g**) GSEA against five H3.3K27M-related gene sets were performed using 2 sets of gene profiles from panobinostat-treated H3.3K27M DIPG cell lines, (**f**) SU-DIPG-VI and (**g**) JHH-DIPG1. The five H3.3K27M-related gene sets were CHAN_NSC_ONLY (genes with H3K27me3 peaks only in NSC line but not SF7761 H3.3K27M DIPG line), CHAN_SF7761_ONLY (genes with H3K27me3 peaks only in SF7761 H3.3K27M DIPG line but not neural stem cell [NSC] line), CHAN_NSC SF7761_OVERLAP (genes with overlapping H3K27me3 peaks in NSC line and SF7761 H3.3K27M DIPG line), BENDER_K27M_UP (significantly up-regulated genes in K27M pHGG tumors compared to WT pHGG tumors) and BENDER_K27_DOWN (significantly down-regulated genes in K27M pHGG tumors compared to WT pHGG tumors). GSEA results showing down-regulation of K27M-induced up-regulated gene sets (CHAN_NSC_ONLY and BENDER_K27M_UP) and up-regulation of K27M-induced down-regulated gene set (BENDER_K27M_DOWN) in panobinostat-treated samples.

Figure S9: Additional in vivo testing

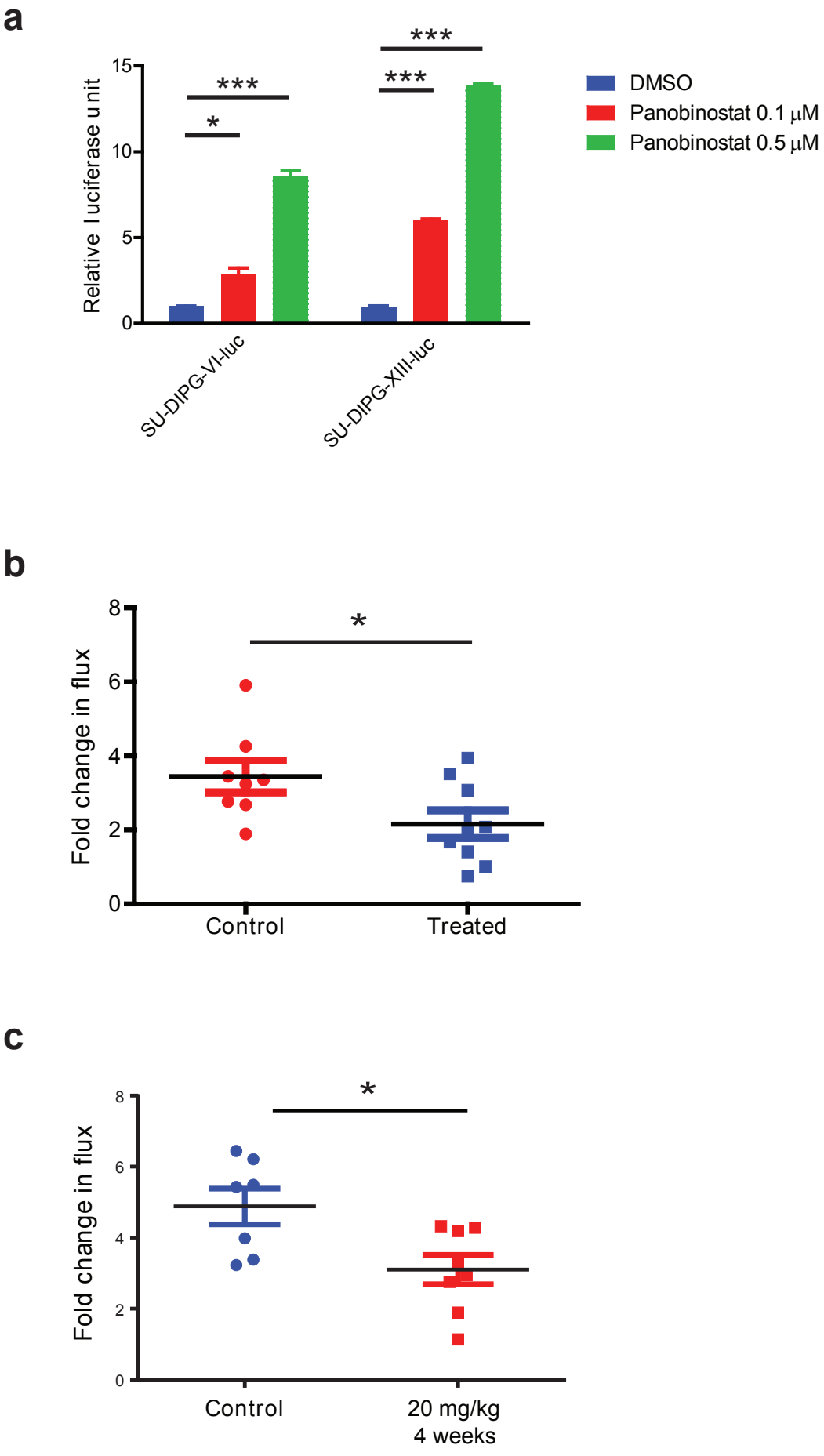

Supplementary Figure 9. Additional *in vivo* testing. **(a)** Luciferase activity change in DIPG-luc lines upon panobinostat treatment *in vitro.* DIPG-luc cells were set in multiple wells of 96-well plate and treated with 0.1% DMSO or panobinostat at 0.1 or 0.5 μM for 48 hours. Then, half of the wells were subjected to the CelltiterGlo assay for assessing cell viability while the other half were subjected to the luciferase assay for assessing luciferase activity. Relative luciferase unit was calculated as the ratio between luciferase activity and cell viability in duplicate or triplicate to assess relative luciferase activity at a per cell level. Data shown as mean ± SD. **P* < 0.05; ****P* < 0.001 (two-tailed t test). (**b**) Replicate experiment demonstrating CED delivery of panobinostat inhibits DIPG orthotopic xenograft growth. As in the experiment described in Fig. 2, NOD-SCID-IL2R-gamma chain deficient mice were implanted with 100,000 SU-DIPG-VI-luc cells in the brainstem at postnatal day 2 (P2) and allowed to engraft for 2 months prior to treatment with a single dose of panobinostat delivered by CED. The data show DIPG xenograft tumor growth *in vivo* as measured by change in bioluminescent photon emission over the seven days following CED delivery of panobinostat (panobinostat group, blue squares) or vehicle control (Control group, red circles). Data points represent fold change in maximum photon flux between Day 0 and Day 7 for each mouse; each data point represents one mouse. n = 8 control, 9 treated mice. Error bars, s.e.m. **P* < 0.05 (two-tailed t test) (**c**) Systemic delivery of panobinostat inhibits tumor growth in a DIPG orthotopic xenograft *in vivo.* SU-DIPG-VI-luc xenograft tumor growth as measured by change in bioluminescent photon emission over 25 days following weekly systemic delivery of panobinostat (panobinostat group, red squares) or vehicle control (Control group, blue circles). Data points represent the fold change in maximum photon flux between Day 0 and Day 25 for each mouse; each data point represents one mouse. In total, four doses of panobinostat 20 mg/kg i.p. were given. n = 7 mice in each group. Error bars, s.e.m. **P* < 0.05 (two-tailed t test).

Figure S10: Resistance to and combination strategies for panobinostat.

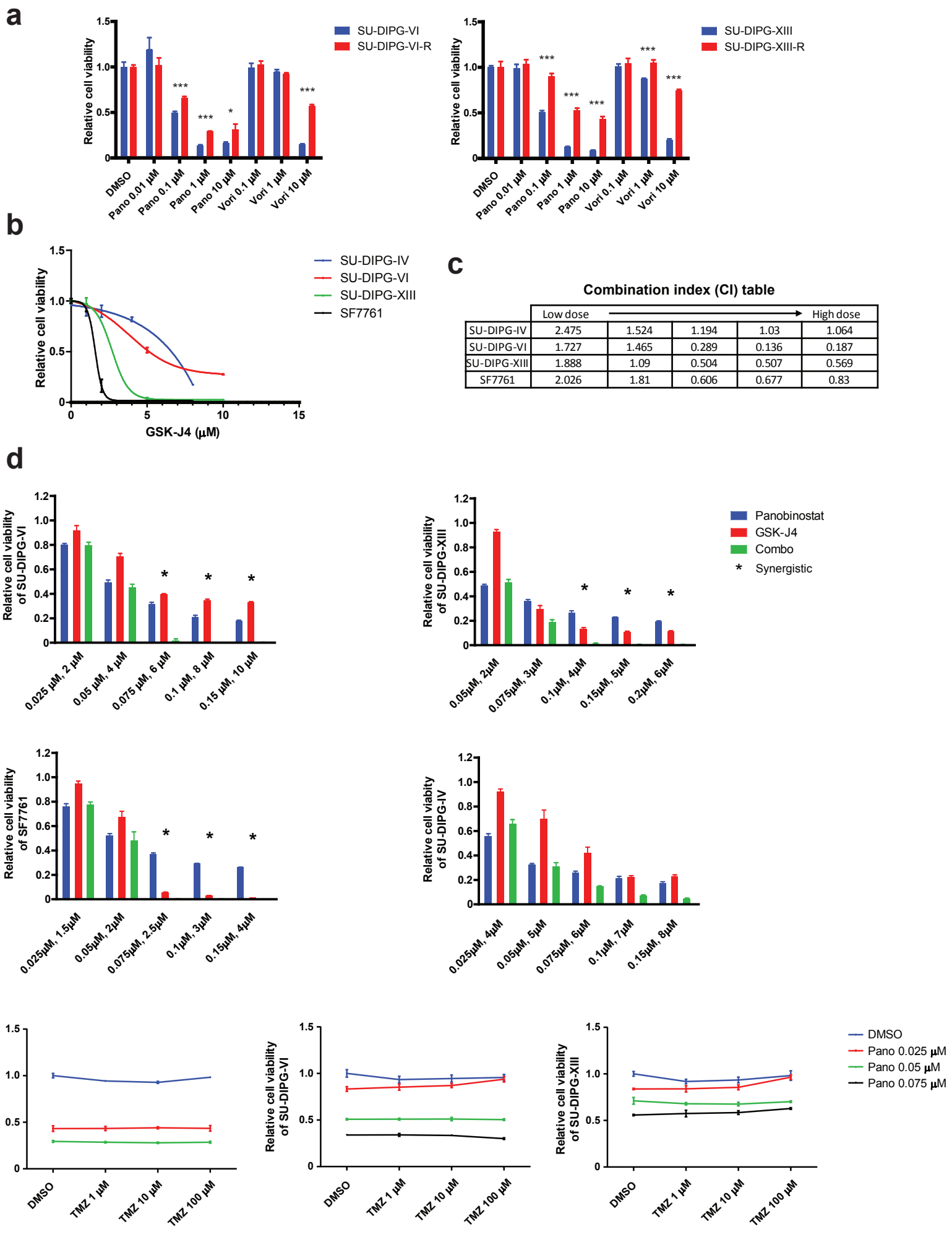

Supplementary Figure 10. Resistance to and combination strategies for panobinostat: (**a**) DIPG cells exhibit resistance to panobinostat with chronic exposure to a sublethal dose. SU-DIPG-VI and SU-DIPG-XIII cells were treated with panobinostat at ~IC50 dose (0.05 μM for SU-DIPG-VI and 0.1 μM for SU-DIPG-XIII) for 3 weeks. The surviving cells (SU-DIPG-VI-R and SU-DIPG-XIII-R) were then seeded in 96-well plates and treated with DMSO, panobinostat or vorinostat as indicated for 72 hr. Parental SU-DIPG-VI and SU-DIPG-XIII cells (not exposed to chronic panobinostat exposure) were subjected to the same treatment in parallel. Cell viability was measured by CellTiterGlo assay relative to 0.1% DMSO control. Data shown as mean ± SD. Two-tailed t test, $*P < 0.05$, $***P < 0.001$ (two-tailed t test). **(b)** Dose response curves of four DIPG cell cultures to GSK-J4 at increasing concentration, measured by CellTiter Glo at 72 hr. (**c**) Summary of combination index (CI) testing of panobinostat and GSK-J4 combination treatment in four patient-derived DIPG cell lines. (**c**) DIPG cells were seeded into 96-well plates and treated with panobinostat and GSK-J4 individually or in combination at the indicated concentrations for 72 hr in at least triplicate. Cell viabilities were then assessed using the CelltiterGlo assay relative to 0.1% DMSO control. Data shown as mean ± SD. *indicates the two drugs demonstrate synergy at that condition (i.e. CI < 1). **(d**) Panobinostat and temozolomide are not an effective combination strategy. DIPG cells were seeded into 96-well plates and treated with panobinostat and temozolomide (TMZ) individually or in combination at the indicated concentrations for 72 hr in at least triplicate. Cell viabilities were then assessed using the CelltiterGlo assay relative to 0.1% DMSO control. Data are shown as mean ± SD. As indicated, temozolomide does not affect DIPG cell viability at concentrations up to 100 μM and panobinostat does not alter the ineffectiveness of temozolomide.

List of Supplementary Tables:

Supplementary Table 1: Clinical and molecular characteristics of DIPG tumors

Supplementary Table 2: STR fingerprints of the DIPG cell lines – Excel file.

Supplementary Table 3: Sequencing statistics and identified mutations – Excel file.

Supplementary Table 4: Calculated combination indices– Excel file.

Supplementary Table 5: Tissue penetration of panobinostat determined by LC-MSMS

Supplementary Table 1: Clinical and molecular characteristics of DIPG tumors

Patient ID	Age at diagnosis/sex	Histology	H3 status	WHO Grade	Treatment	Overall survival	Timing of tissue collection
SU-DIPG-I	5 male	anaplastic astrocytoma	WT	III	XRT (3 days only)	3 mo	autopsy
SU-DIPG-II	7 male	glioblastoma	H3.3-K27M	IV	XRT + temozolomide	12 mo	autopsy
SU-DIPG-III	12 male	diffuse astrocytoma	H3.1-K27M	II	XRT + trisenox	20 mo	autopsy
SU-DIPG-IV	2 female	glioblastoma	H3.1-K27M	IV	XRT + cetuximab/irinotecan	8 mo	autopsy
SU-DIPG-VI	7 female	High-grade glioma	H3.3-K27M	III	XRT + vorinostat	6 mo	autopsy
SU-DIPG-VII	8 male	glioblastoma	WT	IV	XRT (2 days only)	2 mo	autopsy
SU-DIPG-VIII	9 male	anaplastic astrocytoma	WT	III	XRT then XRT + antineoplaston	20 mo	autopsy
SU-DIPG-IX	13 male	high-grade glioma	WT	sample too small to judge	XRT	12 mo	autopsy
SU-DIPG-X	11 male	diffuse glioma	H3.1-K27M		XRT (17 fractions) + vorinostat	1 mo	autopsy
SU-DIPG-XI	5 male	glioblastoma	H3.3K27M	IV	XRT+EGFRVIII vaccine, imetelstat	16 mo	autopsy
SU-DIPG-XII	4 female		H3.3K27M		XRT	7 mo	autopsy
SU-DIPG-XIII	6 female	glioblastoma	H3.3-K27M	IV	XRT	4 mo	autopsy
SK-DIPG27	6	glioblastoma	H3.3-K27M	IV	XRT + bevacizumab, temozolomide		
VU-DIPG.A	3 female	diffuse astrocytoma	H3.3-K27M	II	multiagent chemotherapy		1st month
VU-DIPG.B	4 female	anaplastic astrocytoma	H3.1-K27M	III	XRT		2nd month
Li-A	5	glioblastoma	H3.1-K27M	IV	XRT	17 mo	autopsy
Li-C	13.5	glioblastoma	H3.3-K27M	IV	XRT + renatecan		
Li-D	12	high-grade glioma	H3.3-K27M	III	XRT + valproic acid, avastin		
Li-E	12 female	glioblastoma	H3.3-K27M	IV	(same patient as SU-DIPG-V)		
Li-F	8.5	glioblastoma	WT	IV	XRT-TMZ, Avastin		
OHSU-DIPG#1	4 female	glioblastoma	H3.1-K27M	IV	none (radon mine)	5 mo	autopsy
OHSU-DIPG#2	21 male	glioblastoma	H3.3-K27M	IV	unknown		autopsy
JHH-DIPG1	6 male	glioblastoma	H3.3-K27M	IV	XRT + TMZ/CPT11/bevacizumab	25 mo	autopsy
NEM-157	5 female	oligo-astrocytoma	H3.3-K27M	II	XRT + erlotinib	11 mo	Diagnosis (pre-treatment)
NEM-163	5 male	diffuse astrocytoma	H3.3-K27M	II	XRT + erlotinib	10 mo	Diagnosis (pre-treatment)
NEM-165	3 female	oligo-astrocytoma	H3.3-K27M	III	XRT + erlotinib	15 mo +	Diagnosis (pre-treatment)
NEM-168	9 female	diffuse astrocytoma	H3.3-K27M	III	chemotherapy then RT + erlotinib	8 mo	Diagnosis (pre-treatment)
NEM-175	9	diffuse astrocytoma	H3.3-K27M	II	XRT + erlotinib	15 mo +	Diagnosis (pre-treatment)
NEM-186	3	glioblastoma	H3.1-K27M	IV	XRT (40 Gy hypofractionated)	8 mo	Diagnosis (pre-treatment)
NEM-215	6	oligo-astrocytoma	H3.3-K27M	II	XRT + erlotinib then sirolimus	9 mo	Diagnosis (pre-treatment)
SU-pcGBM-2	15 male	cortical glioblastoma	WT	IV			Diagnosis (pre-treatment)

Legend: XRT = brainstem radiotherapy; WHO = World Health Organization

Tissue	Panobinostat levels
Serum	~ 800 ng/ml of serum
kidney	35.4 ng/mg of tissue
cerebral cortex	0.034 ng/mg of tissue
pons	0.068 ng/mg of tissue (~68 ng/ml)

Supplementary Table 5: Tissue penetration of panobinostat determined by LC-MSMS
A single 20 mg/kg dose was delivered intra-peritoneally in NOD-SCID-IL2 gamma chain-deficient mice, and tissue samples collected 30 minutes later for analysis using liquid chromatography/mass spectrometry (LC-MS/MS). The pontine tissue concentration of 0.068 ng/mg (~68ng/ml) is equivalent to approximately 196 nM. Given that the IC_{50} of panobinostat for the DIPG cell lines is about 100 nM, systemic administration is reasonable in this model.